4-18-2017

Developing Luminescent Lanthanide Coordination Polymers and Metal-Organic Frameworks for Bioimaging Applications

Aida Gonzalez

Xiu Mei-Chu

Kathryn A. Pitton

Ryan Crichton

Jeffrey D. Einkauf

Department of Chemistry and Biochemistry

Developing Luminescent Lanthanide Coordination Polymers and Metal-Organic Frameworks for Bioimaging Applications

Aida Sarita Gonzalez, Xiu Mei-Chu, Kathryn A. Pitton, Ryan Crichton, Jeffrey D. Einkauf & Daniel T. de Lill

This study focuses on the solvothermal synthesis of two lanthanide-based coordination polymer/metal-organic framework systems assembled from 1,3,5-benzenetricarboxylic acid (BTC) in the nano-sized regime for use as bioimaging agents. These materials were synthesized using two different lanthanide ions, a luminescent center (Eu, Tb) for optical imaging purposes and Gd, whose magnetic properties are particularly beneficial in magnetic resonance imaging (MRI) as a contrast agent. Together, these two features allow for multimodal imaging, useful in the study and diagnosis of disease. Under identical reaction conditions, two different compounds were formed upon changing the identity of the optically active lanthanide metal ion. Compound **1** ([EuGd(BTC)$_2$(H$_2$O)$_{12}$]) emerged as a one dimensional coordination polymer, increasing in size with reaction time; while compound **2** ([TbGd(BTC)$_2$(H$_2$O)$_2$]$_n$•2DMF) emerged as a three dimensional framework, decreasing in size with time. Both compounds displayed vibrant luminescence upon UV excitation, indicating potential as bioimaging agents.

• • •

INTRODUCTION

Coordination polymers are described as a compound that joins metal ions through organic moieties (linkers) in one, two, or three dimensions.[1] Metal-organic frameworks (MOFs) are a class of coordination polymers that possess permanent porosity that can be applied in molecular recognition and separation, gas storage, catalysis, sensing, drug delivery, display technologies, luminescence, and biomedical imaging.[1,5,5,11,8] MOFs with luminescence and bioimaging properties in the nanoscale size are currently being studied for promising use in biomedical imaging.[12]

Although MOFs have only been extensively studied for about fifteen years, there are many publications that describe compound synthesis and characterization, with increasing attention on the synthesis of MOFs in the nanometer scale.[12,7] William *et al*. report that the majority of nano-sized imaging entities are constructed by inorganic materials only, including quantum dots, superparamagnetic metal oxides, and gold nanoparticles.[12] MOFs differ from these compounds in not only the presence of an organic component, but also their porosity that can be potentially used for combined imaging and drug delivery, known as theranostics[8].

With an interest in developing MOFs for bioimaging purposes, trivalent lanthanides (Ln) are an ideal selection as the inorganic metal cation in the construction of nanoMOFs (nMOFs). Ln centers allow for multimodal imaging; europium (Eu) and terbium (Tb) provide visible luminescence upon excitation by ultraviolet (UV) radiation, which can be differentiated from natural biological auto-fluorescence due to the relatively long luminescence lifetimes of Ln ions.[9] Lanthanides also possess magnetic properties, especially gadolinium (Gd)

that has seven unpaired electrons. This large number of unpaired electrons creates a large magnetic response that allows for their use as magnetic resonance imaging (MRI) contrast agents.[4] The design of MRI contrast agents requires a magnetic metal ion, one or more coordinated and exchangeable aqua (water) ligands, and high stability in biological media. Currently, the United States Food and Drug Administration (FDA) has only a small number of approved Gd-based MRI contrast agents and developing new and better contrast agents is an active area of research.[3,10] As the ionic radii across the Lns are very similar, it is facile to incorporate several different Ln ions in one material. This feature can provide different functionalities into one compound, such as the aforementioned optical and magnetic properties to produce multimodal imaging. Ln nMOFs can be synthesized with varying numbers of exchangeable aqua ligands, a feature that is good for MRI. Ln nMOF's porosity also provides an alternative platform than current methods for drug loading and delivery that combined with imaging could lead to the development of theranostic nMOFs.

Before nMOFs can be utilized for theranostic applications, however, more fundamental research into nMOF structure-property relationships is necessary. There is still little known about how nMOF structure, composition, dimensionality, particle size, and particle morphology affect imaging properties, particularly concerning MRI. The goal of our research is to understand how these factors contribute to observed luminescent and magnetic responses of nMOF materials. The overall goal of this project is to synthesize nMOFs with both optically and magnetically active Ln ions to produce new multimodal bioimaging agents, and preliminary findings toward this goal are presented herein.

NanoMOFs compounds **1** and **2** were synthesized through the solvothermal reaction of lanthanide salts with an organic linker.[4,6] A 1:2 Eu/Gd (**1**) and Tb/Gd (**2**) system were synthesized, where Eu and Tb allow for optical imaging and Gd brings paramagnetic properties necessary for MRI. It was observed that two different compounds were formed depending on whether Eu or Tb was used during the synthesis, compound **1**= $[EuGd(BTC)_2(H_2O)_{12}]_n$ and compound **2**= $([TbGd(BTC)_2(H_2O)_2]_n \bullet 2DMF)$. (BTC= 1,3,5-benzenetricarboxylic acid, or trimesic acid; DMF= N,N'-dimethylformamide). Synthesis, structure, size control, and luminescent properties will be presented.

SYNTHESIS AND CHARACTERIZATION

Compounds **1** and **2** were synthesized via solvothermal methods in a 23 mL Teflon lined Parr bomb. A 1:2 Ln/Ln (Ln= Eu/Gd or Tb/Gd) mix of the selected lanthanide chloride salts, sodium trifluoroacetate (NaTFA), and BTC were mixed in a ~1:0.9:0.6 Ln:TFA:BTC ratio (21.0 mg of BTC, 0.10 mmol) with the solvents water (H_2O, 4 mL) and DMF (8 mL). The bombs were sealed and heated at 60 °C for 24-72 hours. Once the reactions were completed, the Parr bombs were removed from the oven and allowed to cool to room temperature. After approximately 30 minutes, the bombs were opened and a clear, colorless liquid with a small white solid were observed. The compounds were isolated via centrifugation at 15,000 rpm for 5 minutes, followed by ethanol washes with sonication (five minutes) and allowed to air dry.

Dynamic Light Scattering (DLS) is a technique used for particle size characterization in colloidal dispersions.[6] Once the synthesized samples were cleaned and dried, DLS measurements were performed to estimate nMOF size. Approximately 5-10 mg of nMOF were suspended in an aqueous colloid (~10 mL H_2O) and sonicated for five minutes just before DLS analysis on a Malvern Zetasizer. See Tables 1 and 2 for a summary of nMOF size versus reaction time.

Structural characterization was performed on synthesized nMOFs using powder X-ray diffraction (PXRD) on an Olympus Scientific BTX II Powder X-ray Diffractometer (Co source, 5-55° 2θ). PXRD patterns were matched to known compounds reported in the Cambridge Structural Database (CSD) (Figures 1 and 2) through the Cambridge Crystallographic Data Centre. This is a database of over 800,000 crystal structures reported throughout the literature. This database essentially contains every known crystal structure of compounds containing C-C bonds, with the exception of large macromolecules and biomolecules. PXRD data can be compared to data contained in this database to identify the synthesis of previously reported structures.

Luminescence spectra were collected on a Perkin Elmer LS55 Fluorescence Spectrometer at room temperature (23 ± 2 °C) on both solid samples in a PMMA matrix (2 mg of sample ground in 10 mg of PMMA) and aqueous suspensions (~5-10 mg in ~10 mL DI water followed by 5 minutes of

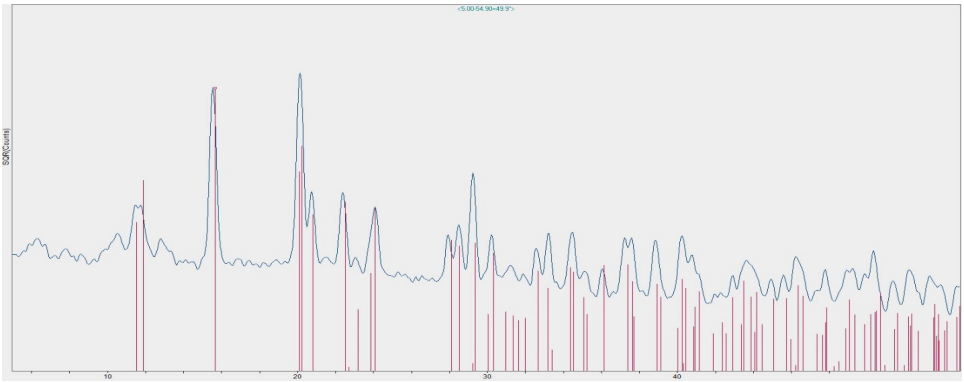

Figure 1. **PXRD pattern (horizontal trace) of** 1 **(reaction time = 48 hours) compared to RAVJUV in the CSD (vertical lines)**

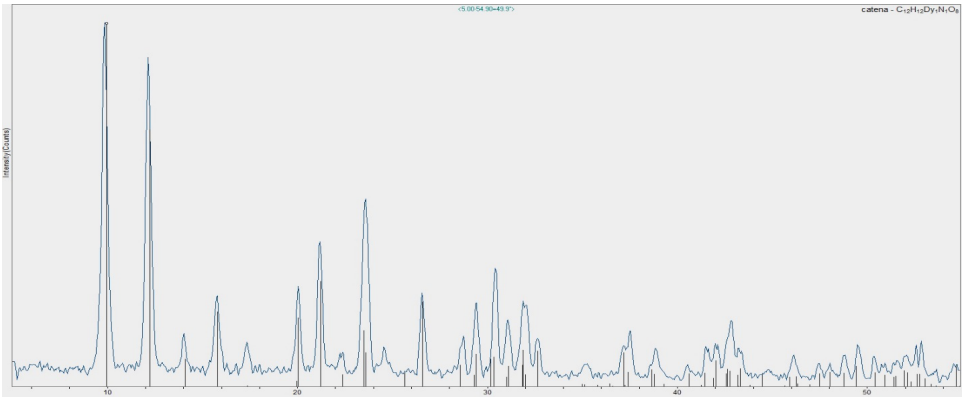

Figure 2. **PXRD pattern (horizontal trace) of** 2 **(reaction time = 48 hours) compared to YEMJAC in the CSD (vertical lines).**

sonication). Excitation spectra were collected at the maximum emission wavelength of Eu (615 nm, **1**) or Tb (545 nm, **2**), and emission spectra were then recorded at the maximum excitation wavelength (~250-300 nm, compound and phase (solid/colloid suspension) dependent).

Preliminary relaxivity data were collected on all compounds, and the data is provided in Table 3. Approximately 0.1 mM aqueous solutions of each nMOF compound were prepared in DI water and sonicated for five minutes. The colloidal suspensions were then placed in a bench top 43 MHz (1T) field Magritek Spinsolve 60 NMR spectrometer. Relaxometry measurements were then conducted to determine T1/T2 relaxation times for each system.

RESULTS

An opposite relationship in particle growth versus time between the two compounds was observed (Tables 1 and 2). Compound **1** depicted particle size increase with time, whereas compound **2** showed an opposite trend decreasing in size with time, and reaching a plateau after 72 hours. PXRD was used to identify compound **1** as RAVJUV and compound 2 as YEMJAC in the CSD.

The 48 hours samples (ASG 2-21 and ASG 1-67) of compound **1** and compound **2**, respectively, were analyzed using fluorescence spectroscopy, and both compounds display vibrant luminescence upon UV excitation (Figure 3) in both the solid state and in aqueous colloidal solutions. The broad excitation profile of **1** and **2** is indicative of absorption of the

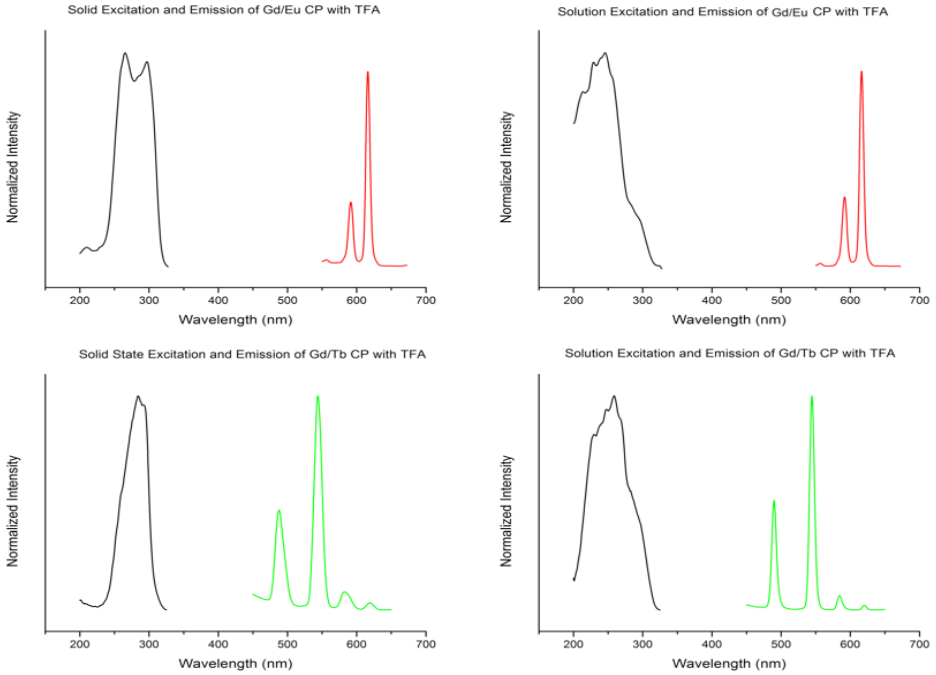

Figure 3. **Excitation (~200-300 nm) and emission (~450-650 nm) spectra of solid (left) and colloidal solutions (right) of** 1 **(top) and** 2 **(bottom).**

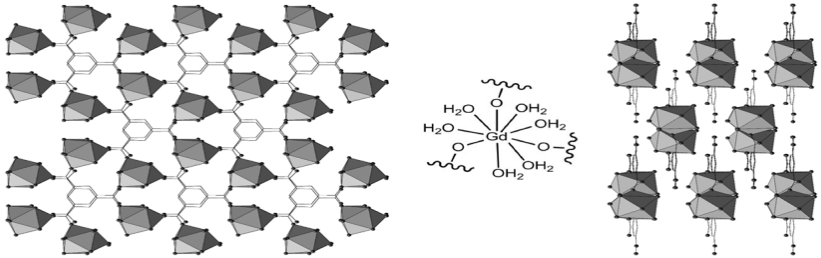

Figure 4. **Structure of compound** 1 **down the [001] direction (left).** Polyhedra represent LnO_9, spheres are oxygen (O) atoms, and black lines are carbon (C) atoms. Hydrogen (H) atoms have been omitted for clarity. Local Ln (Ln = Gd here) coordination sphere is shown in the middle to highlight the six bound water molecules/Ln, and the view down [101] shows the individual chains (right).

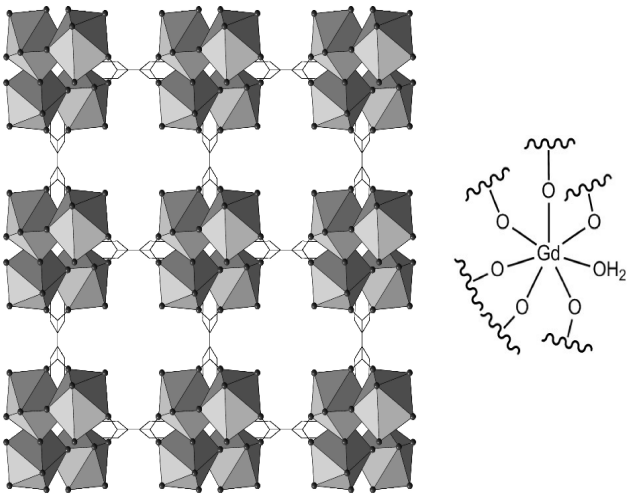

Figure 5. **Structure of compound 2 down [001].** See caption of Figure 4 for atom description details. Note only one bound water molecule/Ln here.

organic BTC component. The BTC absorbs UV radiation and transfers this energy to the Ln ion to sensitize luminescence in a process commonly referred to as the "antenna effect."[2] Upon excitation of the BTC, red Eu and green Tb emission is seen, with minimal background fluorescence from the BTC linker, indicating efficient energy transfer and sensitization. The bright emission is easily seen with the naked eye, essential for use as potential bioimaging agents.

Preliminary measurements of relaxation times (Table 3) indicate that the title compounds do show an increase in relaxation of water protons with relaxivities comparable to those of some currently used Gd-based contrast agents[13], but direct comparisons and consequences of these data require more detailed studies that are planned. Full characterization of the magnetic properties of the compounds have yet to be assessed, however, and will be the focus of future work, as will cell and tissue imaging studies. It is clear though that nMOFs **1** and **2** show promise as MRI contrast agents, though the lack of a clear trend between relaxivity and nMOF size is surprising. This could be due to a combination of size, shape, and/or water diffusion rate effects, but additional studies including electron microscopy will be required to explore this further.

DISCUSSION

The overall purpose of this study was to study nMOF formation and growth in order to assess their use as potential bioimaging and MRI contrast agents. While many MOF structures can be synthesized using any of the lanthanides, in some instances the lighter Lns will produce a different compound than the heavier Lns under otherwise identical reaction conditions. This was observed in the targeted system under study in which Eu/Gd formed a highly hydrated, 1-dimensional compound, and Tb/Gd formed a 3-dimensional, porous framework. This serendipitous discovery was fortunate and provides two contrasting compounds for future imaging studies, one system that contains six water

molecules/Ln center (compound **2**), and the other with one water molecule/Ln center (compound **1**), identical to the MRI contrast agents in current clinical use that consist of Gd-based molecules with one water molecule/Ln.

STRUCTURAL DESCRIPTION

Compound **1** is composed of LnO_9 monomers that extend through fully deprotonated BTC linkers into 1-dimensional chains. The Ln coordination sphere is composed of three monodentate linkages from the deprotonated BTC carboxylate oxygen atoms and six aqua ligands. The chains are densely packed and run parallel to one another in a staggered fashion, shown in Figure 4.

Compound **2** is a three-dimensional framework assembled from LnO_7 polyhedra linked together by fully deprotonated BTC linkers (Figure 5). The Ln is coordinated through monodentate linkages to carboxylate oxygen atoms from six distinct BTC moieties, with one coordinated water molecule to fulfill the coordination sphere. The BTC assemble the monomers into a framework that has residual DMF solvent molecules residing in the pores of the compound (not depicted in Figure 5).

Another interesting observation was the opposite relationship in particle growth versus time between the two compounds (Tables 1 and 2). In **1**, particle size increased with time as expected through typical crystal growth and Oswald ripening processes. The opposite was found to be true in **2**, where particle growth decreased with increasing time. This has been observed in other nMOF systems,[4,14] but is not well understood. This may be due to the differences in dimensionality (1-D in **1** versus 3-D in **2**) between the two systems, but further investigations are required to confirm this conjecture.

CONCLUSION

In conclusion, two nMOFs systems were synthesized and characterized. It was observed that changing the visible emitting Ln ion from Eu to Tb resulted in a significant structural change from a 1-dimensional compound to a 3-dimensional framework. Particle size versus reaction time followed opposite trends, where **1** increased in size over time whereas **2** decreased in size as reaction time increased, contrary to typical nanoparticle crystallization mechanisms. Both **1** and **2** displayed vibrant red and green (respectively) emission upon UV excitation, indicating potential for bioimaging applications. Preliminary relaxometry measurements indicate that the nMOFs show promise as MRI contrast agents, though further characterization is necessary to fully understand the magnetic responses of the compounds. Upon optimization of reaction conditions, nMOFs structure and size were successfully manipulated to provide the materials necessary for future bioimaging studies.

REFERENCES

1.) Batten, S. R.; Champness, N. R.; Chen, X.-M.; Garcia-Martinez, J.; Kitagawa, S.; Ohrstrom, L.; O'Keeffe, M.; Suh, M. P.; Reedijk, J. *CrystEngComm* 2012, *14*, 3001.

2.) Bünzli, J.-C. G.; Piguet, C. Chem. Soc. Rev. 2005, 34, 1048

3.) Comby, S.; Surender, E. M.; Kotova, O.; Truman, L. K.; Molloy, J. K.; Gunnlaugsson, T. Inorganic Chemistry 2014, 53, 1867.

4.) Davies, K.; Bourne, S. A.; Oliver, C. L. Crystal Growth & Design 2012, 12, 1999.

5.) Dey, C.; Kundu, T.; Biswal, B. P.; Mallick, A.; Banerjee, R. *Acta Crystallographica Section B* 2014, *70*, 3.

6.) Guo, X.; Zhu, G.; Li, Z.; Sun, F.; Yang, Z.; Qiu, S. Chemical Communications 2006, 3172.

7.) Jayakumar, M. K. G.; Idris, N. M.; Zhang, Y. Proceedings of the National Academy of Sciences 2012, 109, 8483.

8.) Kuppler, R. J.; Timmons, D. J.; Fang, Q.-R.; Li, J.-R.; Makal, T. A.; Young, M. D.; Yuan, D.; Zhao, D.; Zhuang, W.; Zhou, H.-C. *Coordination Chemistry Reviews* 2009, *253*, 3042.

9.) Na, H. B.; Song, I. C.; Hyeon, T. *Advanced Materials* 2009, *21*, 2133.

10.) Pierre, V.; Allen, M.; Caravan, P. In *Journal of Biological Inorganic Chemistry*; Springer Science & Business Media B.V.: 2014; Vol. 19, p 127.

11.) Ramirez, A. L.; Knope, K. E.; Kelley, T. T.; Greig, N. E.; Einkauf, J. D.; de Lill, D. T. Inorg. Chim. Acta 2012, 392, 46.

12.) Rieter, W. J.; Taylor, K. M. L.; An, H.; Lin, W.; Lin, W. Journal of the American Chemical Society 2006, 128, 9024.

13.) Rohrer, M.; Hans, B.; Mintorovitch, J.; Requardt, M.; Weinmann, H.-J. *Investigative Radiology* 2005, *40*, 715.

14.) Stock, N.; Biswas, S. *Chemical Reviews* 2012, *112*, 933.

15.) Venkataraman, D.; Lee, S.; Moore, J. S.; Zhang, P.; Hirsch, K. A.; Gardner, G. B.; Covey, A. C.; Prentice, C. L. Chemistry of Materials 1996, 8, 2030.

TABLES

Sample Name	Time (hr)	Mean diameter (nm)
ASG 2-11	24	681 ± 34
ASG 2-21	48	1172 ± 253
ASG 2-17	72	1374 ± 104

Table 1. **DLS Results of Compound 1**

Sample Name	Time (hr)	Mean diameter (nm)
ASG 2-7	24	634 ± 24
ASG 1-67	48	562 ± 17
ASG 1-93	72	415 ± 7

Table 2. **DLS Results of Compound 2**

Compound	Sample Name	Size (nm)	T1 (s)	T2 (s)	r_1 ($mM^{-1}s^{-1}$)	r_2 ($mM^{-1}s^{-1}$)
1	ASG 2-11	681	2.85	2.50	3.51	4.00
1	ASG 2-21	1172	2.81	2.27	3.56	4.41
1	ASG 2-17	1374	3.11	2.69	3.21	3.72
2	ASG 2-07	634	2.96	2.51	3.38	2.96
2	ASG 1-67	562	2.89	2.58	3.88	2.58
2	ASG 1-93	415	2.79	2.34	3.58	4.27

Table 3. **Results of relaxometry measurements to produce T1 and T2 relaxation times and relaxivity rates, r1 and r2.**